In and out of the nucleus: CNN based segmentation of cell nuclei from images of a translocating sensor

Tarek M. Zikry
Department of Biostatistics,
University of North Carolina at Chapel Hill
Chapel Hill, NC USA
tarek@live.unc.edu

Katarzyna M. Kedziora
Department of Genetics,
University of North Carolina at Chapel Hill
Chapel Hill, NC USA
kmkedz@email.unc.edu

Michael R. Kosorok
Department of Biostatistics,
University of North Carolina at Chapel Hill
Chapel Hill, NC USA
kosorok@bios.unc.edu

Jeremy E. Purvis
Department of Genetics,
University of North Carolina at Chapel Hill
Chapel Hill, NC USA
purvisj@email.unc.edu

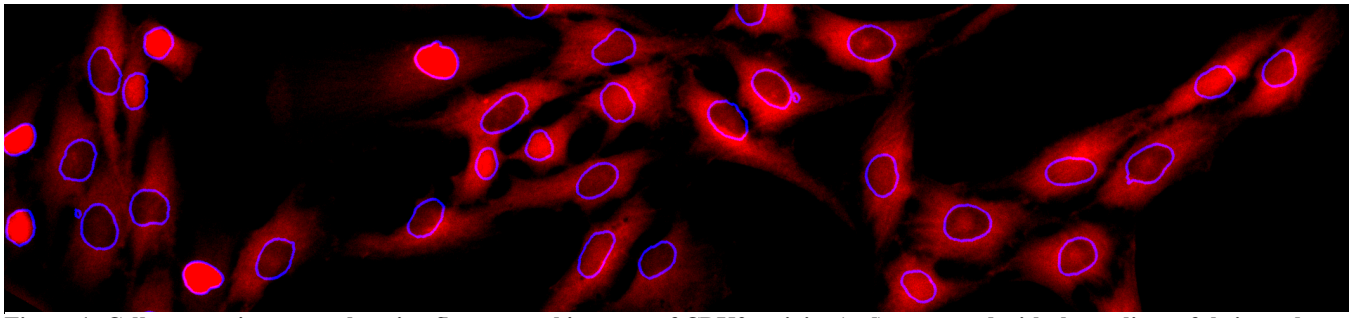

Figure 1: Cells expressing a translocating fluorescent biosensor of CDK2 activity (red) annotated with the outlines of their nuclear regions (blue).

ABSTRACT

This study demonstrates application of convolutional neural networks (CNNs) for the analysis of a unique image analysis problem in fluorescence microscopy. We employed the U-Net CNN architecture and trained a model to segment nuclear regions in images of a translocating biosensor—which alternates between the nucleus and cytoplasm—without the need for a constant nuclear marker. The model provided high-quality segmentation results that allowed us to accurately quantify the extent of cyclin-dependent kinase activity in a population of cells. We envision that the development of this kind of analysis tools will enable biologists to design live-cell fluorescence imaging experiments without the need for providing a constant marker for a subcellular region of interest. As a consequence, they will be free to increase the number of biosensors measured in single cells or reduce the phototoxicity of cellular imaging.

CCS Concepts

• **Computing methodologies → Machine learning approaches; Neural networks;**

Keywords

Deep Learning, Convolutional Neural Network, Segmentation, Fluorescence Imaging, Single Cell, Translocation Biosensors

PEARC '19, July 28-August 1, 2019, Chicago, Illinois, USA

1. INTRODUCTION

With recent advancements in the automation of microscopy experiments, huge quantities of imaging data can be gathered faster than ever before [2]. However, a severe bottleneck has emerged in the difficulty of processing this increasing amount of data. The problem is due to a lack of automated image analysis algorithms providing high quality results in tasks such as image classification, segmentation or object tracking. Recently, deep learning-based image analysis algorithms have emerged as promising new tools to facilitate both automation and extraction of information that is not available to other methods. The strength of this approach lies in the automated extraction of optimal features for each specific image analysis problem, therefore promising a fully customized solution without a need for feature design by experts [8].

Functional imaging of single cells is one of the fast developing bioimaging fields. With the development of new genetically-encoded fluorescent biosensors, one can investigate an increasing number of cellular processes simultaneously in the same cell. One class of functional biosensors contain reporters that provide information on the activity of proteins of interest by localizing to different subcellular compartments. This group is referred to as translocation biosensors [4]. Translocation biosensors often report on the activity of cellular kinases, enzymes responsible for the phosphorylation of other proteins. They play a crucial role in the regulation of cellular signal processing [5]. When a cell is perturbed, functional information such as stimulus intensity and frequency can be encoded in a temporal kinase activation pattern, making kinases a crucial point of research in modern biology [6].

Progression through the cell cycle—one of the most fundamental processes in cell biology—is driven by cyclin-dependent kinases (CDKs). For example, increased activity of Cyclin Dependent Kinase 2 (CDK2) correlates with a cell approaching a new round of DNA replication. Conversely, low CDK2 activity indicates that a cell will withdraw, at least temporarily, from cycles of replication

and division and instead transition to a quiescent state [9]. The CDK2 translocation biosensor is based on a fragment of one of the cellular targets of CDK2, DNA Helicase B, fused to a fluorescent protein tag. When CDK2 is not active, the sensor remains unphosphorylated and localizes to the nucleus. However, when CDK2 becomes active, the sensor translocates to the cytoplasm [9]. Therefore, the cytoplasmic-to-nuclear ratio (Cyt/Nucl) of the sensor fluorescence signal correlates with the activity level of CDK2.

In order to accurately quantify Cyt/Nucl ratio of CDK2 sensor, the nuclear region of each cell must be properly segmented. For the boundary of the nucleus to be delineated correctly, a constant presence of an additional nuclear marker is normally required. However, the presence of an additional nuclear marker in many experiments, especially involving live-cell imaging, can be problematic. The additional marker may increase phototoxicity in an experiment or simply prevent measurements of additional cellular signals by blocking one of the fluorescence channels, which are typically limited to no more than four or five.

However, visual inspection reveals that the CDK2 signal alone should provide enough information to segment nuclei without the use of an additional marker. In cells with low CDK2 activity, the sensor directly marks nuclei. However, as the activity of CDK2 increases, the sensor localizes to the cytoplasm and provides enough contrast to delineate nuclei as elliptical regions devoid of fluorescent signal. We set to employ a deep learning image analysis approach to train a model to segment nuclear regions based solely on the localization signal of the translocating CDK2 biosensor.

Convolutional Neural Networks (CNNs) have proven to be especially apt at image classification and segmentation tasks. Convolution filters are ideal for recognizing localized spatial features and have the added benefit of limiting the number of trainable parameters, reducing computational times to allow for longer training. The U-Net architecture, developed in 2015 for biomedical image segmentation, has been particularly successful in the wide range of image segmentation tasks due to its uniquely symmetric encoding and decoding channels [7].

The goal of this work is to apply U-Net architecture and train a model to segment cellular nuclei in images of CDK2 translocating biosensor without the use a separate nuclear marker.

2. DATA AND METHODS

2.1 Microscopy

RPE-hTert cells expressing CDK2 sensor [9] were cultured on glass-bottom plates (Cellvis, #1.5), fixed with 4% paraformaldehyde for 15 minutes at room temperature and stained with DAPI. Imaging was performed using a Nikon Ti Eclipse inverted microscope using Plan Apochromat dry objective 20x (NA 0.75). Images were recorded using an Andor Zyla 4.2 sCMOS detector with 12-bit resolution and converted to 8-bit before the analysis. All filter sets were from Chroma: DAPI - 395/25 nm; 425 nm; 460/50 nm (excitation; beam splitter; emission filter), mCherry - 560/40 nm; 585 nm; 630/75 nm.

2.2 Dataset

There were 272 CDK2 sensor and DAPI image pairs collected. To create ground truth segmentation masks, the DAPI images were segmented and processed through morphological operations (opening and watersheding) using the SciKit-Image (Skimage) image processing package, version 0.13.1 in Python 3.6. The masks were inspected and corrected manually to avoid erroneously merged objects. To facilitate training, the images were divided into four tiles (1024x1024 px each). The images were divided equally into training and test sets. The training set was then supplemented through data augmentation with 320 additional images.

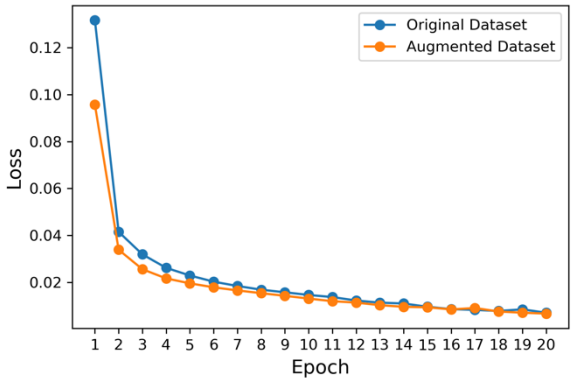

Figure 2: Loss function changes during training.

2.3 Model and training

The convolution neural network architecture U-Net was implemented using the PyTorch machine learning library in Python 3.6. The implementation was adapted from the code from GitHub users jvanvugt [3] and bvezilic [1]. Edge padding was used to eliminate border loss and maintain outputs that match the dimensions of input images. All training and testing was done on a Google Cloud VM instance using an NVIDIA Tesla P100 16GB. A training batch size of two was used and trained over 20 epochs with a learning rate of 0.001 using Adam Optimizer. The binary cross entropy loss function was used to score the model output during training. The changes in the loss function during training using the original and the augmented dataset are shown in Figure 2.

2.4 Evaluation and segmentation

The Jaccard index was calculated for each pair of objects in the ground truth and test images. Jaccard index values were compared with increasing thresholds (in the range from 0.5 to 0.95 with 0.05 increment) to label the objects as true positive (TP), false positive (FP) or false negative (FN). Recall (TP/(TP+FN)) and precision (TP/(TP+FP)) parameters were calculated for each Jaccard index threshold value. In the analysis of recall and precision, the objects were stratified based on CDK2 sensor ratio values defined for true positive objects (in ground truth mask for recall analysis and in model output mask for precision analysis).

Ratios of cytoplasmic to nuclear CDK2 sensor signal were calculated for both the ground truth and model output masks. The cytoplasmic CDK2 sensor level is measured within a 5 pixel-wide ring-shaped region around the nucleus. The distributions of CDK2 sensor ratio values calculated for ground truth and model output masks are plotted in the form of histograms and compared using the 2-sample, 2-sided Kolmogorov-Smirnov test. Scatterplots of CDK2 sensor ratio vs. total DAPI signal within nuclear regions were plotted to compare results obtained using ground truth and model output segmentation masks.

3. RESULTS

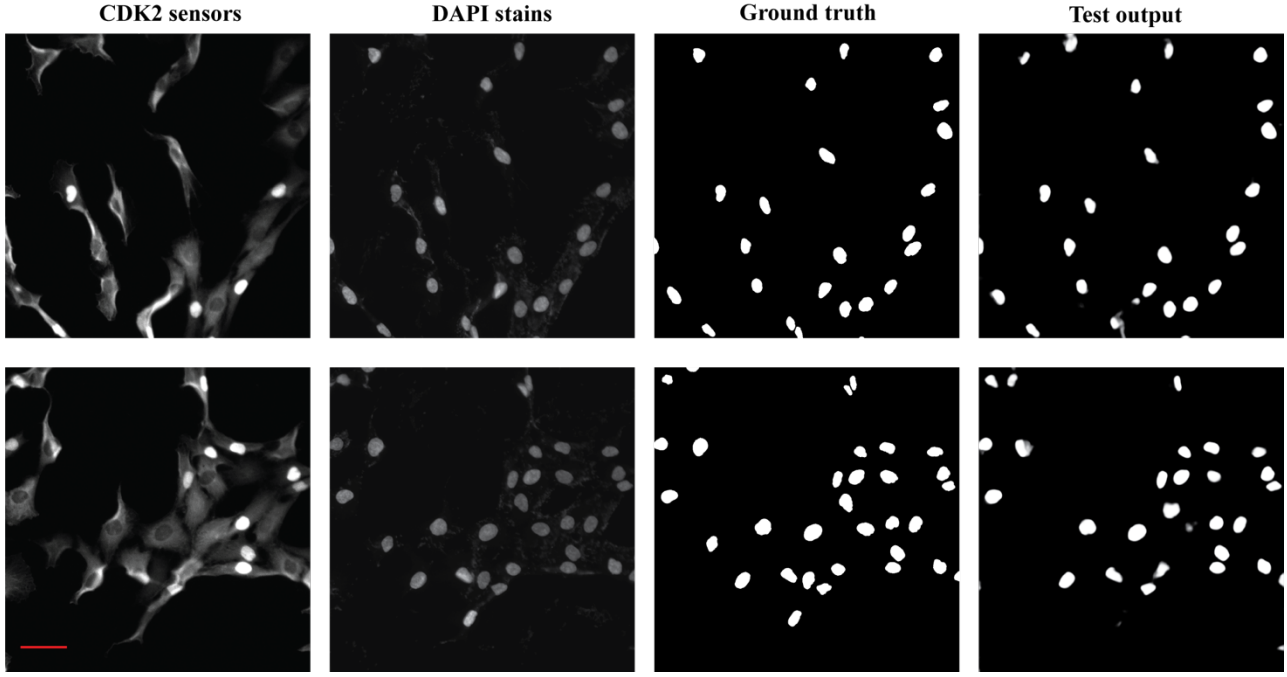

Figure 3:Two examples of fluorescent images (DAPI and CDK sensor) together with the comparison of ground truth segmentation masks and model output for the same fields of view. Scale bar = 50 μm.

Example segmentation results are presented in Figure 3. Visual inspection of the results suggests that the majority of cell nuclei were detected and segmented correctly. However, one can also spot some typical errors of segmentation – missing or misshaped objects and spurious detections.

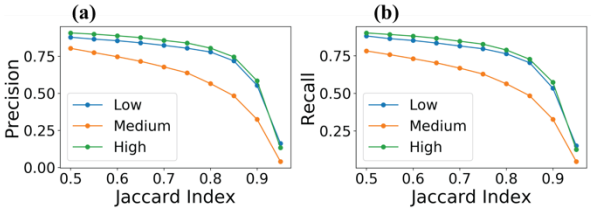

Figure 4: Precision and recall rates calculated based on increasing Jaccard Index threshold values for cells with low, medium, and high CDK2 activity levels.

To quantitatively evaluate the performance of the segmentation, we calculated recall and precision rates of object detection. Positive detection was defined as a pair of objects, whose Jaccard index exceeds a defined threshold value. However, as a single precision and recall score at the specified threshold do not adequately describe the behavior of the model, we repeated the calculation for a range of Jaccard index values. Additionally, we stratified this analysis for groups of cells with different CDK2 sensor cytoplasm over nucleus ratio levels. In the analysis of recall, we used CDK2 ratio values calculated based on ground truth masks. However, in the analysis of precision we had to stratify cells based on CDK2 ratio values calculated based on predicted regions. The results of this analysis are shown in Figure 4. As expected, both recall and precision of detection decrease when a higher value of overlap between the pair of objects is required. Interestingly, both groups of cells with high and low CDK2 ratio levels were detected significantly better than cells with a medium level of CDK2 activity. This result suggests, not surprisingly, that the contrast between the nucleus and the cytoplasm is crucial in proper segmentation of nuclear regions. It is also interesting to note that the cells with high cytoplasm presence of CDK2 sensor were the best performing group over the whole tested range of Jaccard index values.

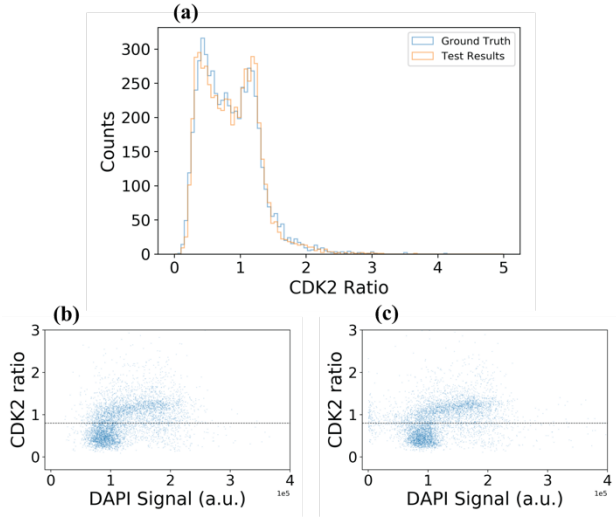

Figure 5: a. Comparison of CDK2 ratio distributions based on ground truth and model output masks. b, c. Total DAPI signal vs. CDK2 ratio for ground truth (b) and predicted nuclear regions (c). Vertical lines indicate arbitrary threshold (at the level of 0.8) between cells positioned early or late in the cell cycle.

Importantly, the segmentation of CDK2 biosensor images allows us to get a quantitative information of the proliferation status of cell colonies. We compared CDK2 activity values calculated based on correct ground truth nuclear region and based on regions detected

by our trained algorithm. The results of this comparison are presented in Figure 5. We do not detect any significant differences in the distribution of CDK2 activity values between the two calculation methods (Kolmogorov-Smirnov test, p=0.46). The percentage of cells with low CDK2 activity value (below threshold level of 0.8) based on ground truth segmentation is 49%. In comparison, the trained algorithm-based segmentation predicted 48% of cells to show CDK2 activity below this threshold level (Figure 5 b and c). This comparison suggests that the quality of segmentation performed by our trained model is sufficient to extract biologically relevant information about the proliferation status of cell colonies.

4. DISCUSSION

In this study we have shown that a U-Net type neural network can be trained to successfully segment nuclear regions based on images of a translocating biosensor. Most notably, the achieved quality of segmentation enables us to calculate the correct distribution of CDK2 activity among cells in a heterogeneous population. This success may be attributed to the fact that the majority of segmentation errors occurs in the population of cells with the intermediate CDK2 activity levels. In these cells, the biosensor is equally distributed between the nucleus and the cytoplasm, providing little contrast for the proper segmentation. Yet consequently, the lack of contrast in this population also results in a limited measurement error of the CDK2 activity, even in case of significant segmentation errors.

There are several possible improvements that may further enhance the segmentation of this class of images. Firstly, by looking at the obtained segmentation results, we observed that one of the most common segmentation errors is detection of two adjacent nuclei as a single object, also known as merging. These errors persisted even after applying an additional watershed segmentation step on the network output. In order to encourage a network to find the missing thin boundaries, the training could be performed using masks with differentially weighted pixels. In such prepared masks, boundaries of close objects should be assigned higher weights than the interior pixels of objects, as implemented in the original U-Net report [7]. Moreover, weighted masks could also be utilized to specifically improve the segmentation of the nuclei of cells with intermediate CDK2 activity and little contrast. Assigning larger weights to pixels belonging to regions with little contrast would effectively force the network to learn how to better segment those regions.

During the analysis of the network results we also noticed that our ground truth segmentation masks contain unexpected errors. Occasionally, cells that were clearly visible in the CDK2 sensor image were entirely missing nuclear signal in the DAPI image. Since the ground truth segmentation was created based on the DAPI images, this led to the overestimation of the number of false positive detections. The lack of consistent DAPI staining may have originated from an unusual error in sample preparation. In the future, a more thorough vetting of the ground truth segmentation images is necessary to avoid this kind of errors compromising the training and confounding the interpretation of the results. Another direction for future improvement of the segmentation results is fine tuning and estimation of hyperparameters in neural network training, for example annealing of the learning rate during training or testing different loss functions. Finally, we were successful in improving the performance of the network by using data augmentation and adding transformed images to our training set. This approach could be exploited further and multiple transformations could be added to the training set.

In future work, we plan to test and fine tune our model in segmentation of live cell time lapse imaging data which require fully automated high throughput analysis methods. We will also address the question of robustness by testing how transferable the trained model is between images collected with slightly different experimental settings and between images of different kinds of cells expressing the same translocating biosensor.

5. CONCLUSIONS

In this paper, we present a successful application of deep learning for segmentation of images of cells expressing the CDK2 activity biosensor, which translocates between the nucleus and cytoplasm. Using the U-Net CNN architecture, we showed that cellular nuclei can be segmented from CDK2 biosensor images alone without use of any additional biological reporters. This research serves as a proof of concept for the application of deep learning methods in the analysis of microscopy images of cells missing fluorescent marker directly localizing to the organelles of interest.

6. ACKNOWLEDGMENTS

Our thanks to Juanita Limas from UNC-Chapel Hill for a gift of hTert-RPE cells expressing fluorescent biosensors and UNC Information Technology Services for providing access to computational resources.

7. REFERENCES

[1] bvezilic. 2018. Nuclei-segmentation. https://github.com/bvezilic/Nuclei-segmentation.

[2] Daniel L Coutu and Timm Schroeder. 2013. Probing cellular processes by long-term live imaging–historic problems and current solutions. *J Cell Sci* 126, 17 (2013), 3805–3815.

[3] jvanvugt. 2019. pytorch-unet. https://github.com/jvanvugt/pytorch-unet.

[4] Shirley K Knauer, Sabrina Moodt, Thorsten Berg, Urban Liebel, Rainer Pepperkok, and Roland H Stauber. 2005. Translocation biosensors to study signal-specific nucleo-cytoplasmic transport, protease activity and protein–protein interactions. *Traffic* 6, 7 (2005), 594–606.

[5] Takamasa Kudo, Stevan Jeknić, Derek N Macklin, Sajia Akhter, Jacob J Hughey, Sergi Regot, and Markus W Covert. 2018. Live-cell measurements of kinase activity in single cells using translocation reporters. *Nature protocols* 13, 1 (2018), 155.

[6] Jeremy E Purvis and Galit Lahav. 2013. Encoding and decoding cellular information through signaling dynamics. *Cell* 152, 5 (2013), 945–956.

[7] Olaf Ronneberger, Philipp Fischer, and Thomas Brox. 2015. U-net: Convolutional networks for biomedical image segmentation. In *International Conference on Medical image computing and computer-assisted intervention*. Springer, 234–241.

[8] Dinggang Shen, Guorong Wu, and Heung-Il Suk. 2017. Deep learning in medical image analysis. *Annual review of biomedical engineering* 19 (2017), 221–248.

[9] Sabrina L Spencer, Steven D Cappell, Feng-Chiao Tsai, K Wesley Overton, Clifford L Wang, and Tobias Meyer. 2013. The proliferation-quiescence decision is controlled by a bifurcation in CDK2 activity at mitotic exit. *Cell* 155, 2 (2013), 369–38.